Journal of Aerospace Technology and Management
ISSN: 1984-9648
editor@jatm.com.br
Instituto de Aeronáutica e Espaço
Brasil

Araujo Machado, Humberto
Simulation of Ablation in a Composite Thermal Protection System via an Interface Tracking Method
Journal of Aerospace Technology and Management, vol. 4, núm. 3, julio-septiembre, 2012, pp. 331-340
Instituto de Aeronáutica e Espaço
São Paulo, Brasil

Available in: http://www.redalyc.org/articulo.oa?id=309426159009

How to cite
Complete issue
More information about this article
Journal's homepage in redalyc.org

Scientific Information System
Network of Scientific Journals from Latin America, the Caribbean, Spain and Portugal
Non-profit academic project, developed under the open access initiative

doi: 10.5028/jatm.2012.04030312

Simulation of Ablation in a Composite Thermal Protection System via an Interface Tracking Method

Humberto Araujo Machado*
Instituto de Aeronáutica e Espaço - São José dos Campos/SP – Brazil
Universidade do Estado do Rio de Janeiro - Resende/RJ - Brazil

Abstract: *In this work, the two-dimensional computational simulation of the ablative process in a composite used in rocket thermal protection systems via an interface tracking method was presented. The ablative model considers the presence of two simultaneous moving fronts, the pyrolysis and char fronts. The results were compared with some experimental data, showing better agreement than the one-front model. Such procedure will allow a more accurate dimensioning of rocket thermal protection systems, contributing for project optimization.*

Keywords: *Ablation, Composite, Moving boundary, Computational simulation.*

LIST OF SYMBOLS

Cp	Specific heat at constant pressure
K	Thermal conductivity
L	Heat of ablation/melting/pyrolysis
q	Heat flux
T	Temperature
t	Time
V	Interface velocity
Y	Tangential coordinate
ε	Emissivity
ρ	Density
σ	Boltzman constant

INTRODUCTION

Aerodynamic heating in space and suborbital vehicles is a consequence of the hypersonic flight within the atmosphere, i.e., below 100 km of altitude. Depending on the velocity and trajectory, the air temperature around the nose top may surpass 2000ºC at the stagnation point (Machado and Pessoa Filho, 2007a, b). In such situation, aerodynamic heating plays a very important role in the vehicle design. Besides the high temperatures effects on the mechanical behavior of the structure and onboard devices, it is mandatory to preserve the payload, by using an efficient thermal protection system (TPS). TPS design is a critical aspect of the rocket design, since its under dimensioning may result in the loss of the payload and the over dimensioning implies in increasing weight and cost. Along the years, ablative materials have been effectively used as TPS of space vehicles. In these processes, the kinetic energy of the rocket is converted into heat, which consumes the TPS through ablation (Rogan and Hurwicz, 1973). It is a complex phenomenon related with diverse simultaneous physical processes (Silva, 2001).

The ablation is usually calculated through simplified models that consider a single-phase change at constant temperature. Such approach is not always applicable, and may become greatly inaccurate (Machado and Pessoa Filho, 2007a, b). Also, the characterization of the ablative properties under this approach is difficult, since it presents different values for different processes of measurement (Da Costa *et al*., 1996). The study of the ablative processes can be grouped in three categories: engineering models, numerical methods (computational fluid dynamics – CFD, direct simulation Monte Carlo – DSMC, etc.), and experimental methods. The two last demand great investment of time and resources. The first is recommended in the initial stages of space vehicles development.

The coupling between heat transfer processes in the surface and within the layers represents an additional difficult. The external heat exchange occurs by convection and radiation, and the heat transfer to the wall (TPS and structure) happens by conduction. The convective heat transfer coefficient can be estimated through some engineering methods, based on empirical results. In order to obtain the temperature

Received: 18/01/12 Accepted: 22/06/12
*author for correspondence: humbertoham@iae.cta.br
Pç. Mal. Eduardo Gomes, 50. CEP: 12.228-901 - São José dos Campos/SP – Brazil

profile and the heat load, the energy conservation equation has to be solved. A common approach is to consider the heat conduction as one-dimensional, in the normal direction relative to the local surface. However, such hypothesis becomes inaccurate as temperature gradients in the tangential direction, the change of material or a great thickness variation occur (Mazzoni *et al*., 2005). As an example, the TPS of the SARA suborbital platform, which has been developed by the Institute of Aeronautics and Space (IAE), shown in Fig. 1, represents a typical situation in which the one-dimensional approach may result in an appreciable deviation in the temperature distribution and ablation profile. It is remarkable that, in this case, a small deviation in the surface geometry due to ablation may result in a considerable increase in the reentry trajectory uncertainty.

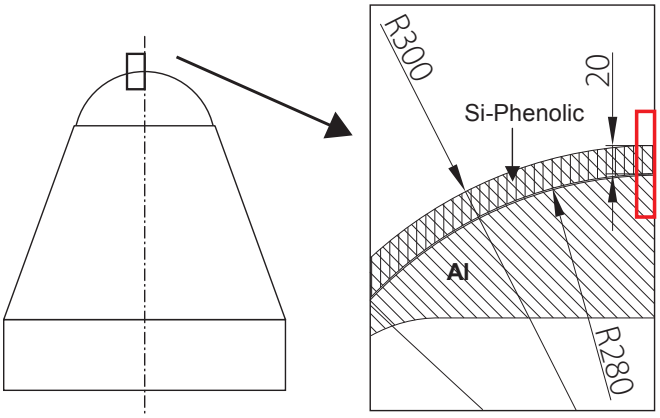

Figure 1. The SARA suborbital platform profile and its TPS in detail.

The full calculation using a discrete method implies great computational effort, including grid generation and solution of a boundary-moving problem. An alternative to these options may be the use of the interface tracking method, proposed by Unverdi & Tryggvason (1992), which allows obtaining a solution for the coupled ablation-conduction problem in the whole domain, considering the full physical model.

The objective of this work was to present a computational simulation of the ablative process via the interface tracking method, applied to a multilayer ablative model. Such procedure will allow applying more complex models for ablation, taking into account the presence of several ablative and structural layers, and providing a more accurate TPS dimensioning.

PHYSICAL PROBLEM

In this work, the ablation model proposed for a composite material considered the presence of two layers: the virgin material and the char layer, which appears after the pyrolysis front. Two moving fronts were accounted: the pyrolysis and the ablation front of the char layer. Both appeared at constant and specific temperatures. The hypotheses considered for the mathematical model were:

- solid materials are isotropic with constant properties;
- the pyrolysis front is considered to have zero thickness, and the pyrolysis reaction happens at constant temperature and enthalpy;
- char layer recession is supposed to occur due to oxidation or sublimation at constant temperature;
- absence of melting layer;
- the resulting gases fully react and perfectly mix with the external air layer, without influence over its properties;
- air is considered a perfect gas;
- radiation is absorbed or emitted by the external surface, however it is not transmitted.

When a heat flux is imposed to the external surface, the TPS warms as a pure transient heat conduction problem until the ablation temperature is reached. Once the TPS surface reaches the ablation temperature, its thickness is reduced; therefore, a transient and coupled problem of heat conduction and moving boundary appears.

The set of equations used to represent the physical problem is written according to the interface tracking method (Juric, 1996). The TPS and the air around it are represented as parts of a continuous domain of calculation. The application of the energy conservation principle to an infinitesimal volume element of the mathematical domain leads to a partial differential equation for the temperature, namely Eq. 1:

$$\frac{\partial(\rho \cdot C_p \cdot T)}{\partial t} = \nabla \cdot K \nabla T + Q \tag{1}$$

where K is the thermal conductivity, and Q is a source term that takes into account the net heat exchange at the boundary (Eq. 2):

$$Q = \int_A q\delta(x - x_f)\,dA \tag{2}$$

where x is the position in the coordinate system, $\delta(x - x_f)$ is a Dirac delta function, which is non-zero only at the interface position,

x_f, dA is a surface element of the interface, and

q is the source term of energy per surface unit of the interface. One should note that this term might exist in every moving interface.

For the external (char) layer, this would be as in Eq. 3:

$$q = \rho LV + q_e + \varepsilon\sigma[T_F^4(t) - T_\infty^4] \quad (3)$$

where,
V is the interface velocity,
T_F is the interface temperature,
T_∞ is the external temperature,
L is the heat of ablation, and
q_e is the prescribed external heat flux.

For the pyrolysis front, it is simplified as in Eq. 4:

$$q = \rho L_P V \quad (4)$$

where L_P is the pyrolysis heat.

Also, the mass flux of resulting gases is neglected, due its low density (when compared to the solid material). Indeed, the specific mass in Eqs. 3 and 4 is the interface density, which was obtained from the mean average of the two phases separated by this front.

Although the air is included in the domain, this region is considered adiabatic, and the heat capacity and thermal conductivity are assumed to be null. Once ablation or pyrolysis temperatures are reached, the temperature jump condition becomes (Eq. 5):

$$T_F = T_A = 0 \quad (5)$$

where T_A will be the ablation or the pyrolysis temperature, according to the interface.

Solution Method

The moving boundary problem was solved by the interface tracking method introduced by Unverdi & Tryggvason (1992), and employed by Juric (1996) in solving phase change problems. In this method, a fixed uniform Eulerian grid is generated, where the conservation laws are applied over the complete domain. The interface acts as a Lagragean referential, where a moving grid is applied. The instantaneous placement of the interface occurs through the constant remeshing of the moving grid, and each area of the domain is characterized by the indicator function, which identifies the properties of the wall and the air around it.

This method allows representing any geometry used in the TPS, and also the characterization of every layer separately. It is accomplished without high increase in the computational cost and does not need any preprocessing (construction of unstructured grid or coordinate transformation). In this work, this method is employed to estimate the ablative performance of the TPS, considering a two-dimensional approach in both, the heat conduction and the moving boundary problem.

Interface tracking method for one moving interface

The interface is represented as a parametric curve, $R(u)$, where the normal and tangent vectors and curvature are extracted. The interface points are interpolated by a Lagrange polynomial, which allows to obtain the geometric parameters and remeshes the curve, keeping the distance d between curve points within the interval $0.9 < d/h < 1.1$, where h is the distance among the fixed grid points, as shown in Fig. 2.

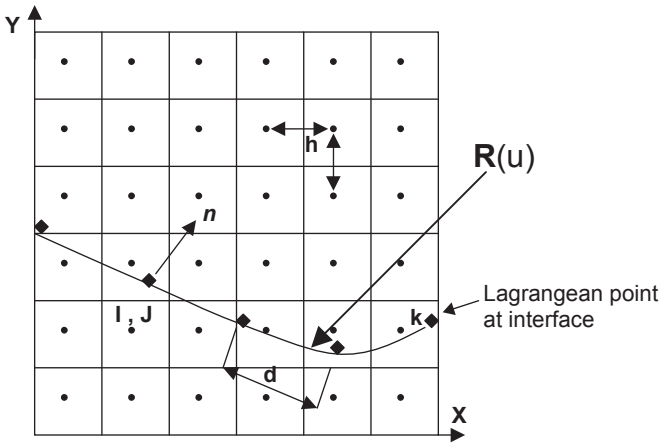

Figure 2. Eulerian and Lagrangean meshes.

The indicator function is used to represent the different phases. For the simple case of only two phases, it varies from 1 (air) to 0 (solid), and is it numerically constructed using the interface curve to determine a source term $G(x)$. The jump of the indicator function across the interface is distributed over the fixed grid points, yielding a gradient field in the mesh (Eq. 6):

$$G(x) = \nabla I = \int_A n\delta(x - x_f)\,dA \quad (6)$$

where n is the normal unitary vector, and the term $\delta\ (x - x_f)$ should be zero, except over the interface, as represented by the Dirac delta function, δ.

However, such representation is not convenient for a discrete number of points, since the Lagrangian points, x_k, do not necessarily coincide with the Eulerian grid points, $x_{i,j}$. The distribution function is used to represent the interface discontinuity as a continuous and smooth function. Such function is similar to the Gaussian distribution one and its value depends on the distance $|x_{ij} - x_k|$ between the Lagrangean and Eulerian points (Eq. 7):

$$D_{i,j}(x_k) = \frac{f[(x_k - x_i)/h].f[(y_k - y_j)/h]}{h^2} \tag{7}$$

where D_{ij} is the distribution function for a point k in the Lagrangean mesh with respect to an Eulerian point (x_i, y_j). One should note that increasing h results in a thicker interface.

The function f is the probability distribution, Fig. 3, related to the distance h as Eq. 8a and b:

$$f(x) = \begin{cases} f_i(x) & if\,|x| \le 1 \\ 1/2 - f_i(2 - |x|) & if\ 1 |x| < 2 \\ 0 & if |x| \ge 2 \end{cases} \tag{8a}$$

$$f_i(x) = \frac{3 - 2.|x| + \sqrt{1 + 4.|x| - 4x^2}}{8} \tag{8b}$$

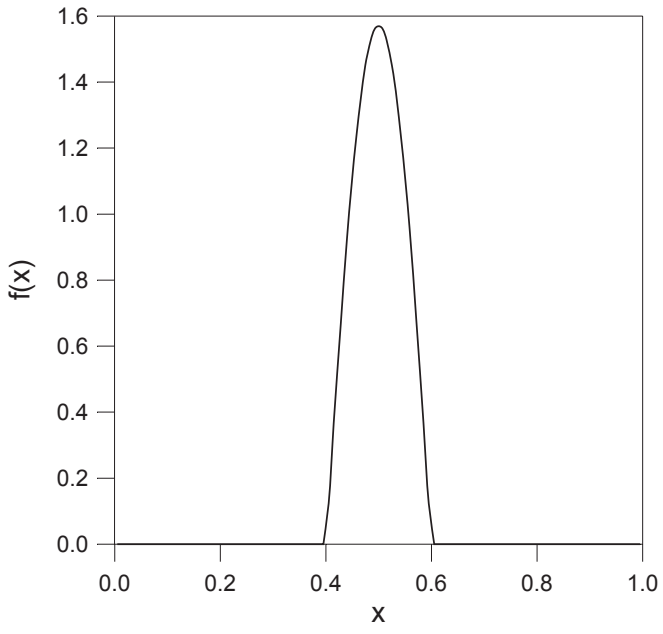

Figure 3. Probabilistic distribution profile.

The divergence of the gradient field is found by numerical derivation of Poison's equation (Eq. 9):

$$\nabla^2 I = \nabla . G \tag{9}$$

Despite being considered constants in each phase, the properties inside the domain must be treated as variables in the formulation. A generic property ϕ(ρ, Cp or K) is expressed as (Eq. 10):

$$\phi(x) = \phi_0 + (\phi_1 - \phi_0) I(x,t) \tag{10}$$

where ϕ_0 and ϕ_1 are the property values for phases 0 and 1 (according to their values of indicator function), respectively.

The coupling between the moving mesh and the fixed grid is done at each time step, through the distribution function, which is used to represent the source terms in the balance equations and to interpolate the fields with infinitesimal discontinuities into a finite thick region at the interface. In a similar manner, this function is used to interpolate the field variables from the Eulerian grid to the interface. The equations used to distribute the source term in the field and interpolate variables to the interface are Eqs. 11 and 12:

$$Q_{i,j} = \sum_k q_k D_{i,j}(x_k) . \Delta s_k \tag{11}$$

$$T_k = \sum_{i,j} h^2 T_{i,j} D_{i,j}(x_k) \tag{12}$$

where Δs_k is the average of the straight-line distances from the point k to the two ones on either side of $x_{k,}$ and corresponds to the area concerned to the point x_k in the interface surface. Equation 11 is the dicretized form of Eq. 2, in which the Dirac delta function was replaced by the distribution function, $D_{i,j}$, which is also done in Eq. 6.

The initial interface shape, $R(u)$, is first specified and then the indicator function is constructed. From the initial conditions, the property and temperature fields are determined. Out of the ablative period, the interface temperature is kept below the ablation one, and the energy equation is solved as a pure heat conduction problem, via the finite volume method, employing an explicit time-marching schedule.

As the interface reaches the ablation temperature at a given point, an iterative process starts up, in order to determine the interface velocity at each time step, which must satisfy the temperature condition (Eq. 5), at that interface point. The process goes on as far as the point temperature is equal to the ablation temperature. The steps to be followed are:

1. Using the current value of V (result for the previous time step), the interface points are transported to a new position, calculated explicitly through the equation $V^n = (dx_f / dt).n$, where n is the normal unitary vector;
2. Density and specific heat are calculated at the new interface position;
3. V^{n+1} is estimated via Newton iterations, using a numerical relaxation schedule (Eq. 13);
4. Heat flux q crossing the interface is calculated through Equations 3 or 4, depending on the interface, and distributed into the fixed grid through Eq. 11;
5. According to the boundary conditions, energy equation (Eq. 1) is used to obtain the temperature at time step $n+1$;
6. Temperature is interpolated to find T_F at the interface, using Eq. 12;
7. The temperature jump condition is tested and if it is lower than the reached tolerance, the fields of viscosity and conductivity are updated for the new position, and one step in time is advanced. If that is not the case, a new estimate for V^{n+1} is calculated and the process returns to step 5.

The convergence criterion used in step 7 is the residual in Eq. 5. Once it has reached the desired tolerance, convergence for interface velocity is assumed. Otherwise, the velocity is corrected via Newton Iterations, given as Eq. 13:

$$V^{n+1} = V^n - \omega.R(T) \tag{13}$$

where ω is a relaxation factor, and $R(T)$ is the residual for the temperature jump condition at the interface. Iterations are repeated until $R(T)$, in every point, becomes smaller than the prescribed tolerance. The optimum value for ω is found by tentative at the calculation beginning.

The method was compared with the analytical solution for a simple phase change problem (Ruperti Jr., 1991), resulting in an excellent agreement, as it can be seen in Fig. 4. Small oscillations in data points are consequences of the visual extraction of the points.

Extension to various moving interfaces

When there is more than one interface, an indicator function, I_m, is created for each one in order to characterize every region concerned to the interfaces individually. Therefore, in a region m (that corresponds to a specific phase or material), a generic property is estimated as Eq. 14:

$$\phi = \sum_{m=1}^{NFC} \phi_m Ig_m \tag{14}$$

where NFC is the number of interfaces. The Lagrangean grids for all interfaces have the same values for the parameters h and d, shown in Fig. 1, and are constructed from a particular parametric curve $R_m(u)$. Ig_i is the global indicator function for a region m, obtained from the indicator function of each interface (calculated as described before). It is given as Eq. 15a and b:

$$Ig_m = I_{m-1} - I_m \tag{15a}$$

$$I_0 = 1; I_{NFC} = 0 \tag{15b}$$

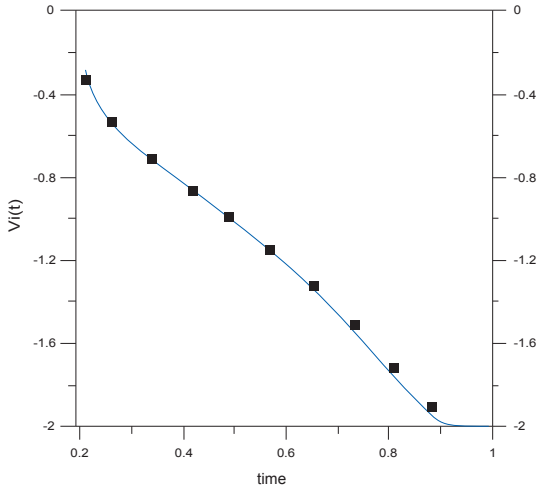

(a) Dimensionless ablation velocity with dimensionless time

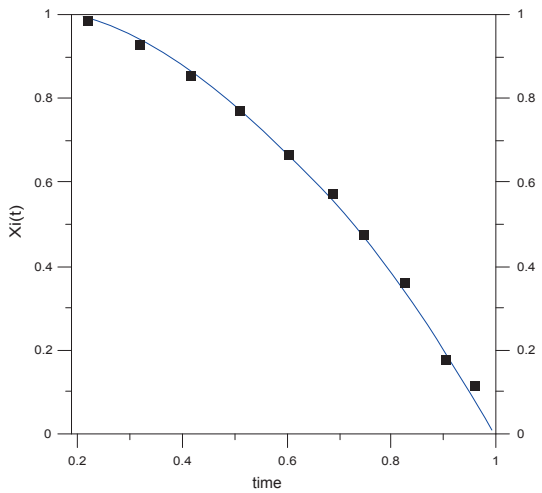

(b) Dimensionless interface position with dimensionless time

Figure 4. Comparison between results of Ruperti Jr. (1991) and interface tracking method for one-dimensional ablation.

If there are more than one moving interface, the source term Q_m for every interface has to be extracted from a modified form of Eq. 2 (Eq. 16):

$$Q_m = \sum_k \int_A q_m \delta_m (x - x_{Fm,k}) dA_m \quad (16)$$

Actually, according to the numerical method, Eq. 11 will be used to calculate the source term in every interface. The total amount of heat generated will be the summation of heat sources of all interfaces (Eq. 17):

$$Q = \sum_m Q_m \quad (17)$$

The convergence criterion and velocity correction are the same as that for the case of one interface, but they are extended to all interfaces at each time step. It must be pointed out that, although a different Lagrangian mesh is necessary for each interface, a unique Eulerian mesh is used, and applied in Eq. 12 for every interface.

RESULTS AND DISCUSSION

The computational code was employed to simulate a one-dimensional ablation process, alike that conducted by Barros (2008), in which material samples were exposed to a plasma jet and had their temperature and heat flux measured.

The ablation was simulated using the two-fronts model presented in this work and the traditional model of one front, where the moving front problem was solved via a pure Lagrangean method (Machado and Pessoa Filho, 2007a, b; Machado, 2006). The main objective was to compare the accuracy of both models, with one and two moving fronts, and to verify the performance of the two moving fronts approach. In this study, the target was not a perfect match between experimental and theoretical data, but the qualitative behavior of the physical approach, in order to verify its coherence and the upgrade in the simulation of the physical problem when the more complete physical model is used.

The mass loss rate was the parameter chosen in order to compare experimental data and numerical results. During the experiment, the mass loss rate was evaluated comparing the sample mass after a period of exposure to the plasma jet. The rate was obtained dividing the mass loss by the time of exposure. The same process was employed to obtain the mean mass loss rate in the simulations. However, the calculation of the mass loss rate was done instantaneously through the integration at each time step, while the experimental method showed the final result after the selected period.

The material used in the samples was the quartz-phenolic resin (Si-Phenolic). The fraction of resin was not specified in the work of Barros (2008), varying from 42 to 31% (results from thermogravinometric analysis). Samples were flat cylinders, with thickness of 10 mm and diameters of 12 and 30 mm. The properties used in the simulation are presented in Table 1.

Table 1. Properties of the quartz-phenolic resin

Property	One-front model	Two-front model	
		Virgin	Char
K (W/mºC)	0.485 [1]	0.485 [1]	0.428 [4]
Cp (J/kgºC)	1256 [1]	1256 [1]	879.5 [4]
ρ (kg/m^3)	1730 [1]	1730 [1]	1300 [4]
ε	0.8 [1]	0.8 [1]	0.8 [5]
Heat of ablation (MJ/kg)	12 [2]	-	-
Ablation temperature (ºC)	538º [2]	-	-
Heat of pyrolysis (MJ/kg)	-	0.78 [3]	-
Pyrolysis temperature (ºC)	-	599º [3]	-
Heat of melting/sublimation (MJ/ kg)	-	-	10.5 [5]
Melting temperature (ºC)	-	-	3700º [5]

[1] Da Costa et al. (1996); [2] Gregori et al. (2008); [3] Tick et al. (1965); [4] Williams and Curry (1992); [5] Savvatimskii (2003).

The one-dimensional heat conduction problem was solved considering prescribed heat flux in the warmed face and adiabatic surface in the opposite one, as boundary conditions. The initial temperature was 27ºC (300 K).

Heat fluxes of 0.44631, 0.64262, 0.89933, 1.21644, and 2.18289 MW/m^2 were imposed to the warmed face. According to Barros (2008), the heat flux over the surface was controlled by the power of the plasma torch and its distance from the sample surface, and the result uncertainty in the evaluation of heat fluxes varied from 0.03 to 0.08 MW/m^2, depending on the heat flux value.

The simulations with the one-front model were done with a six-point grid along the thickness. The simulations with the two-front model were done in a 12 mm thickness dominium of calculation (10 mm for the ablative layer and 2 mm for the air layer) and 5 mm of length. A 24 × 10 points Eulerian grid was employed, resulting in a ten-point Lagrangean mesh, parallel to the interface direction, unless for the maximum value of the heat flux, when a dominium of 12 × 1.5 mm and a 40 × 5

points grid were used.

In Fig. 5 the mass loss rates are presented along the time of exposure to the plasma jet (flame) for each value of the prescribed heat flux. The one-front model highly overestimates the values, when compared to the experimental results. The two-front model slightly underestimates these values, although it is closer to experimental data. For the minor values of heat flux, the initial shapes of the curves obtained from the numerical simulations are far from the experimental results. It might be a consequence of the numerical treatment, since in both numerical methods the ablation velocity tends to infinite at the instant when ablation starts. Since the integration is done at every time step, the relative weight of this initial period becomes important in the result for the low-heat fluxes, because the stabilization of the process takes more time in these cases. It is also important to consider the different ways the rates are calculated.

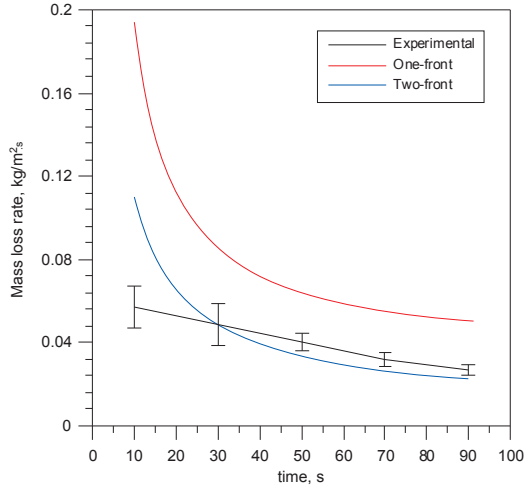

(a) 0.45 MW/m²

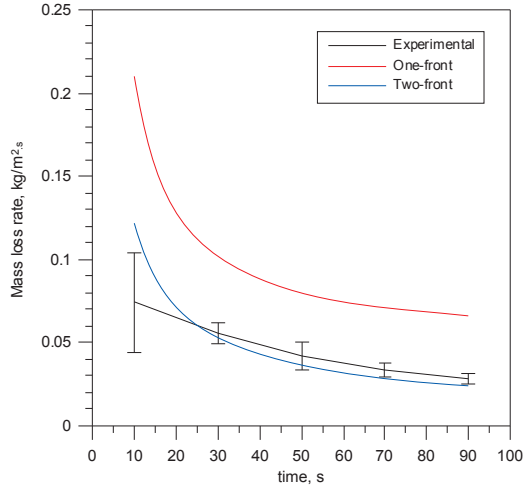

(b) 0.64 MW/m²

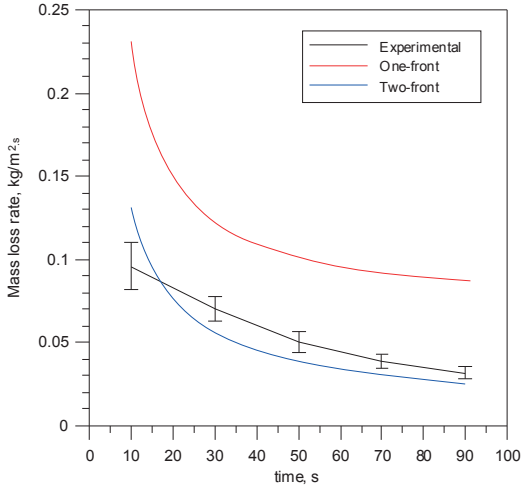

(c) 0.90 MW/m²

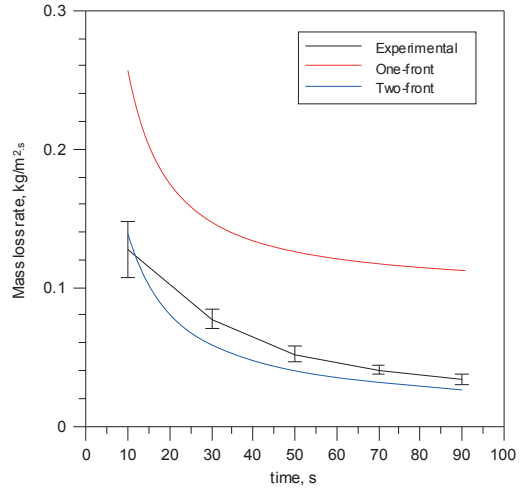

(d) 1.33 MW/m²

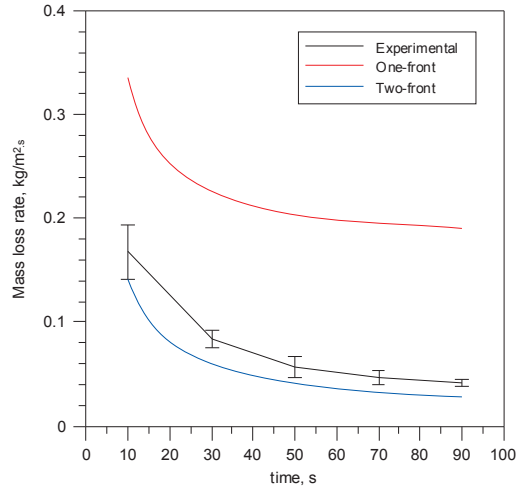

(e) 2.18 MW/m²

Figure 5. Results for one and two-front models compared with the experimental data (Barros, 2008) for the mass loss rate with the time of exposure to the flame.

The measurements are done in finite intervals, while the numerical rates are calculated instantaneously, at each time step. However, for the major values of heat flux, all of them present the same behavior (curve shape).

The root mean square (*rms*) error was used as a measurement of the agreement between the results and is defined as (Eqs. 18 and 19):

$$rms = \sqrt{\frac{\sum_{i=1}^{n} \Delta m_i^2}{n}} \tag{18}$$

$$\Delta m_i = \frac{m_e - m_s}{m_e} \tag{19}$$

where m_e and m_s refer to the mass loss rates extracted from Barros (2008) and from the computational simulation, respectively.

Table 2 shows a clear advantage of the two-front model, a reduction that exceeded 80%.

Table 2. Comparison of *rms* for both models.

Case	*Q* (MW/m²)	*rms* Two-front	*rms* One-front
1	0.45	0.45	1.26
2	0.64	0.31	1.26
3	0.90	0.25	1.30
4	1.33	0.20	1.61
5	2.18	0.28	2.56
Total *rms*	-	0.31	1.67

Figure 6 shows the external surface temperature extracted from the simulation with the two-front model, compared to the experimental measurements (Barros, 2008). Temperature uncertainty was not available in the reference, and all data for the experimental results were collected visually. Although final values present an increasing discrepancy with the heat flux imposed, the behavior is similar, which attests the physical coherence of the mathematical model used in the simulations. Table 3 shows the temperatures when steady state is reached and once again evidences the improvement in the agreement when models are compared. The one-front model considers that the external surface should be at a constant ablation temperature, and the two-front one considers the external temperature of the char layer, which might be exposed to the air. If the absolute values (in Kelvin) of the final temperatures are considered, the average deviation in the absolute temperature falls from -48.6

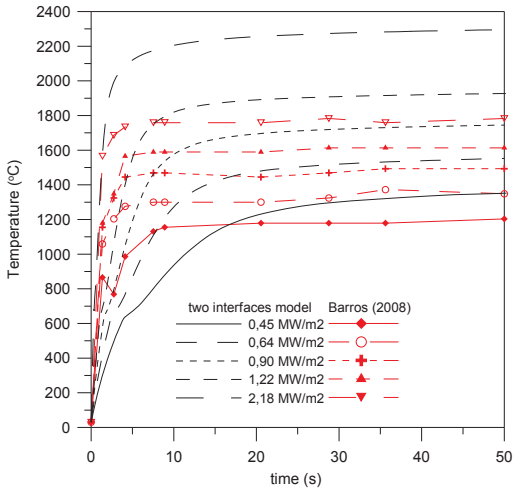

Figure 6. Results for the two-front model compared with the experimental data (Barros, 2008) for the surface temperature with the time.

Table 3. Final surface temperatures.

Case	Experimental[1]	One-front[2]	Deviation (%)[3]	Two-front[4]	Deviation (%)[3]
1	1167ºC	538ºC	-39.4	1389ºC	+ 15.0
2	1312ºC	538ºC	-44.9	1579ºC	+16.8
3	1433ºC	538ºC	-48.8	1766ºC	+19.5
4	1590ºC	538ºC	-53.1	1943ºC	+19.0
5	1747ºC	538ºC	-56.8	2312ºC	+28.0
		Average	-48.6	Average	+19.7

[1] Barros (2008), after 50 seconds; [2] Ablation temperature; [3] Experimental value taken as reference, in K; [4] After 100 seconds.

to +19.7%, which is a reduction of almost 60%.

In Fig. 7 the temperature profile at the final time (90 seconds) is shown for the case of maximum heat flux. The position of the external surface keeps constant, since the melting temperature of the char is not reached. The displacement

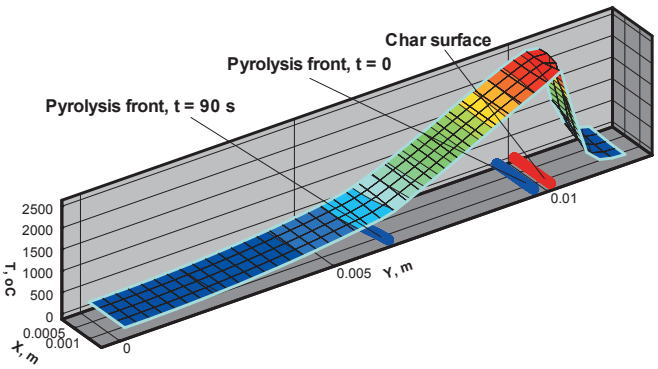

Figure 7 Temperature profile at 90 seconds with initial and final positions of each front, for a heat flux of 2.18289 MW/ m².

occurs in the pyrolysis front (considered being initially at 0.1 mm from the external surface, only for calculation). The temperature gradient is greater in the char than in the virgin material, confirming its effect as a thermal insulator. The external surface temperature (about 2500ºC) is vastly superior to the pyrolysis or to the ablation ones for the one-front model.

When comparing the performance of both models, some aspects of the results should be accounted, such as the uncertainty of the experimental results, the simple approach used in their construction (that neglects the influence of various physical processes), and values of the properties used in the calculation, which were extracted from several sources and consequently are subject to different evaluation conditions. Despite all these aspects, the two-front model can be considered more accurate than the one-front model.

CONCLUSIONS

In this work, a two-front model for ablation in composites used in TPS was employed to simulate the one-dimensional ablation process by a plasma jet. The results were compared with the traditional one-front model and with experimental data extracted from literature. Results showed that the two-front model is more accurate than the one-front model, despite of its simplicity. The numerical solution behavior of the two-front model has demonstrated physical coherence, despite of not perfectly matching the experimental data collected from the selected reference, which was not the objective of this work as mentioned. These results confirm its higher accuracy when compared to the one-front model.

The moving boundary problem was simulated via interface tracking method. The results demonstrated that the method is capable of capturing the temperature peak and of representing the ablation process as a moving boundary problem, in the presence of more than one single layer. Results shall be extracted for more refined meshes, in order to check the method accuracy.

This analysis can be applied to diverse regions of the rocket, more layers, and other shapes. A more realistic physical model for the ablation in the composite material may now replace the simple one used in this work. The inclusion of the flow field effects, like injection of mass due to sublimation, shall also be incorporated into the simulation. In future works, the effect of temperature variation in the pyrolysis, accounted through the Arrhenius equation, should be included.

ACKNOWLEDGEMENTS

The author would like to thank the *Conselho Nacional de Desenvolvimento Científico e Tecnológico* (CNPq), the Brazilian Federal Agency for Science and Technology, for their financial support during this work.

REFERENCES

Barros, E. A., 2008, "Thermal Plasma for Ablation in Materials Used in Heat Shield of Space Systems" (In Portuguese), M.Sc. Dissertation, ITA, São José dos Campos, Brazil. 170p.

Da Costa, L. E. V. L. *et al*., 1996, "Viability Study of Thermal Protection for SARA Platform" (In Portuguese), IAE/CTA, Technical note NT-130-ASE-N/96, IAE/CTA, São José dos Campos, Brazil.

Gregori, M. L. *et al*., 2008, "Properties of Quartz-Phenolic Composites for Thermal Protection Systems", 59th IAC Congress, Glascow, Scotland.

Juric, D., 1996, "Computations of Phase Change", PhD Thesis, University of Michigan, Michigan. 166p.

Machado, H. A., 2006, "Thermal Protection for Aerodynamic Heating of the SARA Sub-orbtial Platform" (In Portuguese), CONEM 2006, Recife, Brazil.

Machado, H. A. and Pessoa-Filho, J. B., 2007a, "Aerodynamic Heating at Hypersonic Speeds", Proceedings of 19th Brazilian Congress of Mechanical Engineering, Brasília, Brazil.

Machado, H. A. and Pessoa-Filho, J. B., 2007b, "Aerodynamic Heating on VSB-30", ESA Symposium, Visby, Sweden.

Mazzoni, J. A. and Pessoa Filho, J. B., Machado, H. A., 2005, "Aerodynamic Heating on VSB-30 Sounding Rocket", Proceedings of 18th Brazilian Congress of Mechanical Engineering, Ouro Preto, Minas Gerais, Brazil.

Rogan, J. E. and Hurwicz, H., 1973, "High-temperature Thermal Protection Systems, in Handbook of Heat Transfer", edited by Rohsenow, W. M., Hartnett J. P., McGraw-Hill, New York, section 19.

Ruperti Jr., N. J., 1991, "Solution of a One-Dimensional Ablation Model" (In Portuguese), M.Sc. Dissertation, National Institute for Space Research – INPE, São José dos Campos, Brazil. 100p.

Savvatimskii, A. V., 2003, "Melting Point of Graphite and Liquid Carbon", Physics-Uspekhi, Vol. 46, No. 12, pp. 1295 - 1303.

Silva, D. V. F. M. R., 2001, "Estimative of Thermal Properties of Ablative Materials" (In Portuguese), M.Sc. Dissertation, Federal University of Rio de Janeiro - UFRJ, Rio de Janeiro, Brazil. 108p.

Tick, S. J. *et al.*, 1965, "Design of Ablative Thrust Chambers and Their Materials", Journal of Spacecraft & Rocket, Vol. 2, No. 3, pp. 325-331.

Unverdi, S. O. and Tryggvason, G., 1992, "A Front-Tracking Method for Viscous, Incompressible, Multi-fluid Flows", Journal of Computational Physics, Vol. 100, pp. 25-37.

Williams, S. D. and Curry, D. M., 1992, "Thermal Protection Materials – Thermophysical Property Data", NASA Reference Publication 1289.